Journal of Materials Chemistry

Cite this: J. Mater. Chem., 2012, 22, 23650

www.rsc.org/materials

PAPER

Dual length-scale nanotip arrays with controllable morphological features for highly sensitive SERS applications†

Hwan Chul Jeon,[a] Sung-Gyu Park,[b] Soojeong Cho[a] and Seung-Man Yang*[a]

Received 9th July 2012, Accepted 24th September 2012
DOI: 10.1039/c2jm34470j

Hexagonally ordered, dual length-scale nanotip arrays were fabricated using a combination of prism holographic lithography, reactive ion etching, and electron-beam evaporation. Double layered, face-centered cubic structures were prepared using prism holographic lithography and were used as templates for the nanotip arrays. The morphological features of the nanotip arrays were easily controlled in the subsequent etching process by varying the etching time and etchant gases. The surfaces of the nanotips were covered with, and roughened by, small protrusions. The nanotip arrays showed tunable surface-enhanced Raman scattering activities that depended on the sharpness, shape, and surface roughness. The simple tunability and high sensitivity of these nanotip arrays make them very promising as a high-fidelity sensing platform.

Introduction

Surface-enhanced Raman scattering (SERS) is a powerful technique for the detection and analysis of numerous molecules at very low concentrations.[1,2] The nanoscale distances between metal nanoparticles, and the sharp edges of metal nanostructures, can function as 'hot-spots' that result in the enhancement of electromagnetic (EM) fields, due to localized surface plasmon resonance (LSPR);[3–16] these features are therefore important in generating a highly sensitive SERS response. In attempts to achieve more highly enhanced Raman signals (which represent the spectral peaks of characteristic molecular structures),[1,2] much work has been dedicated to the fabrication of roughened metallic SERS substrates with a large number of 'hot-spots', using sophisticated fabrication techniques.[1–16] However, the production of uniform SERS platforms with high sensitivity over large areas is still a major challenge for wider and practical sensing applications.

Meanwhile, prism holographic lithography (HL) uses the optical interference of coherent light beams to fabricate defect-free, large-area periodic nanostructures in a simple and rapid manner.[3–5,17–21] The crucial disadvantages of conventional multi-beam HL—which include the complexity of aligning the optical setup needed to control the optical path lengths, and reconfiguration[22–24]—are easily overcome in prism HL, which uses novel prisms to create multiple beams from a single laser beam.[3–5,17–21] HL-featured polymeric nanostructures have great potential for various applications, including photonic applications[5,22–24] and microfluidic sensing and mixing applications.[19,20] Recently, we also have demonstrated the potential of the HL-derived nanostructures either as metal deposition or milling masks for the production of original metal nanostructures or as freestanding 3D porous templates for electroless deposition of the metal nanoparticles.[3–5]

In this paper, we report a facile method for the fabrication of hexagonally ordered, dual length-scale, large-area nanotip arrays with controllable morphological features; this method uses prism HL-derived 3D periodic structures as sharpened and roughened templates for directional or isotropic metal deposition. The sharpness and overall geometrical shape of the polymeric nanotip arrays (which were derived from HL-featured double layered face-centered cubic (FCC) structures) could be controlled to give morphologies ranging from triangular pyramidal tips to more sharpened, conical tips. This was achieved by adjusting the reactive ion etching (RIE) time, using SF_6 gas as the etchant. After directional silver (Ag) deposition, the resulting metallic nanotip arrays showed highly sensitive SERS responses, with tunability depending on the morphological features. Additional O_2 RIE resulted in polymeric nanotip arrays with a smaller-scale surface-roughness. The sensitivity of the SERS signals generated from these dual length-scale nanotip arrays was further increased with large-scale structural homogeneity. The enhancement was found to result from both the sharpened tips and the roughened surfaces, which were featured with sub-15 nm gaps between the adjacent Ag nano-trenches after the isotropic deposition of the thin Ag film. Furthermore, the roughened regions of the dual length-scale nanotip arrays also showed potential as a fluorescence-based sensing platform.

[a]*National CRI Center for Integrated Optofluidic Systems, Department of Chemical and Biomolecular Engineering, KAIST, Daejeon, 305-701, Korea. E-mail: smyang@kaist.ac.kr; Fax: +82 42-350-5962*
[b]*Korea Institute of Materials Science, 797 Changwondaero, Seongsangu, Changwon, Gyeongnam, 642-831, Korea*

† Electronic supplementary information (ESI) available: SEM images and SERS spectra of the resulting periodic metallic nanostructures using prism HL. See DOI: 10.1039/c2jm34470j

Experimental

Fabrication of the dual length-scale nanotip arrays

The fabrication procedure used to produce the sharp nanotip arrays consisted of three main steps; prism HL, RIE, and metal deposition. An SU-8 photoresist (PR) was spin-coated onto the glass wafer with a thickness appropriate for the fabrication of 2-layer FCC structures; this was achieved by controlling the PR resin concentration and the spin speed.[3,4] Large-area, uniform arrays of 2-layer FCC structures were achieved *via* HL, using a previously reported optical setup, and a specially designed top-cut prism.[3,4,19–21] The resulting polymeric nanostructures were then etched using 13.56 MHz RF RIE equipment (Vacuum Science). SF_6 gas was introduced into the chamber at a flow rate of 100 sccm, and etching was performed at an RF power of 100 W for various etching times. During the etching process, the 3D surface morphology of the resulting polymeric structures changed because of the different polymeric density distribution (see Fig. S1, ESI†).[21,25] Finally, a 50 nm Ag film was directionally deposited on the polymeric nanotip arrays, using electron-beam evaporation. To obtain the desired nanoscale roughness on the surfaces of polymeric nanotip arrays, O_2 RIE was performed for 30 s after SF_6 RIE, at a flow rate of 100 sccm.[6] The isotropic deposition of a thin Ag film (10 nm) was then carried out, using multi-sputtering to maximize the roughness enhancement effect (for the process diagram, see Fig. S2, ESI†).

Measurements and characterization

The morphologies of the surface and cross-section of the samples were investigated by field emission-scanning electron microscopy (Hitachi S-4800). The Raman spectra were recorded using a high-resolution dispersive Raman microscope (Horiba Jobin Yvon, LabRAM HR UV/Vis/NIR), in which a 785 nm laser with a power of 75 mW was focused on the sample surface with a beam diameter of 1 μm. The rhodamine 6G (R6G) fluorescence image was obtained by using a Zeiss LSM510 laser scanning confocal microscope (Carl Zeiss Inc.), with a 543 nm He–Ne laser.

Results and discussion

Fig. 1a shows a large-area scanning electron microscopy (SEM) image of a hexagonally ordered polymeric nanostructure array with extremely sharp tips, after 3 min SF_6 RIE processing, using a double layered FCC structure. From the SEM image, we confirmed that the nanotip arrays were uniformly well-ordered in a hexagonal pattern, without defects. The average tip diameter in the polymeric nanotip arrays was determined to be 46 nm, using SEM inspection. The geometrical features of the metallic nanostructure arrays could be changed by adjusting the etching time after the directional deposition of a 50 nm Ag film, as shown in Fig. 1b–e. As the etching time was increased to 2 min, the volume fraction of the bridges connecting each nanotip motif in the as-prepared FCC structures decreased (Fig. 1b and c). After 3 min of etching, the polymeric density was reduced, the bridges became disconnected, and finally, nanotip arrays with sharp tips were produced. As the etching time was increased from 3 min to 4 min, the average tip diameter in the resulting metallic nanotip arrays became smaller (3 min = 78 nm, 4 min = 42 nm).

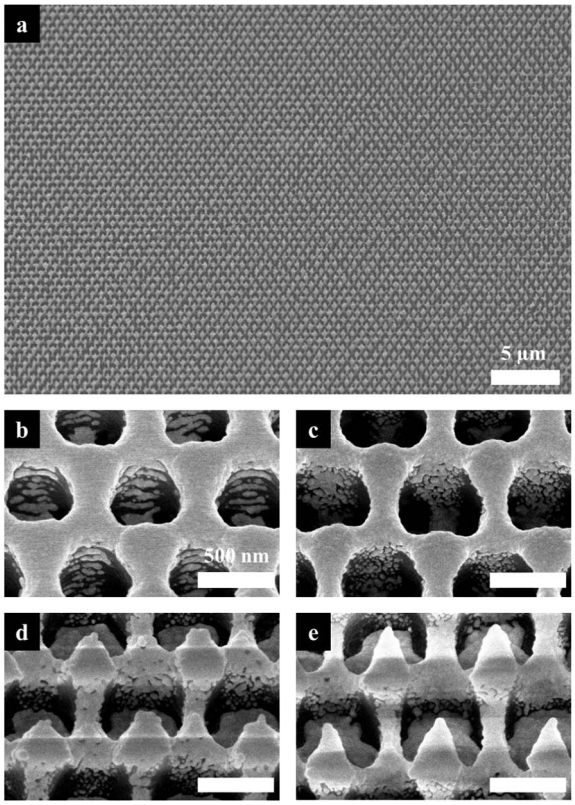

Fig. 1 (a) Large-area SEM image of hexagonally ordered nanotip arrays produced after 3 min of the SF_6 RIE process, using a 2-layer FCC structure. 30° tilted SEM images of the feature-controlled nanostructure arrays, after a directional Ag-deposition step using (b) 0 min, (c) 2 min, (d) 3 min, and (e) 4 min etched 2-layer FCC structures, respectively.

Furthermore, the overall geometrical shape of the resulting nanotip arrays was also changed after 4 min of etching, compared with that observed after 3 min of etching. From the top-view SEM images of the resulting metallic nanostructures reproduced in Fig. 2, we could observe that the size of the elliptical holes in the 2-layer FCC structures became larger resulting from the decrease in the volume fraction of the bridges

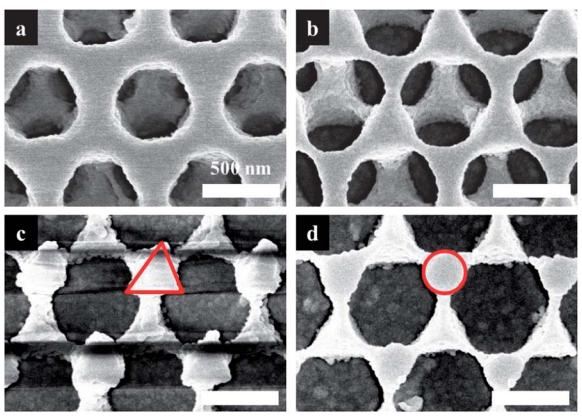

Fig. 2 Top-view SEM images of the feature-controlled nanostructure arrays after a directional Ag-deposition step using (a) 0 min, (b) 2 min, (c) 3 min, and (d) 4 min etched 2-layer FCC structures, respectively.

during initial 2 min of etching (see Fig. 2a and b). After disconnecting the bridges from each motif, the top portions of the 4 min etched nanotips showed a circular shape, whereas those in the 3 min etched case showed a triangular shape, as shown in Fig. 2c and d. Therefore, the overall geometrical shape of the nanotips in the arrays changed from a triangular pyramidal shape to a sharper conical shape as the SF_6 etching duration was increased.

To test the potential of the prepared metallic nanotip arrays as sensor platforms, the SERS performances were measured using a high-resolution dispersive Raman microscope. The surfaces of the prepared metallic samples were exposed to benzenethiol (BT) probe molecules (which have characteristic peaks at 994, 1017, 1071, and 1571 cm^{-1})[3–5] *via* immersion for 6 h in 2 mM ethanolic BT solution. After repeated washing with ethanol, Raman spectra were collected over a period of 5 s, using a 785 nm laser with a power of 75 mW. Fig. 3 shows the SERS spectra of BT adsorbed onto four different SERS substrates produced using various SF_6 etching times; the spectra were compared with that obtained from a smooth flat Ag film as a reference. The characteristic BT peaks were not observed for the flat Ag film. The intensity of the Raman signals obtained from the as-prepared substrates increased as the SF_6 etching time was increased from 0 min to 3 min, but was decreased for the substrate with an SF_6 etching time of 4 min.

Such SF_6 etching duration-dependent variations in the Raman performance can be attributed to the transition of the structural features of the various SERS substrates. For the as-prepared raw FCC substrate (Fig. 1b), the roughened periodic Ag hole arrays on the polymeric template, and the small gaps between the Ag nanoparticles deposited onto the side-walls of the polymeric template, could function as 'hot-spots'. However, this process was inefficient and there were few gaps,[3,4] leading to a low SERS intensity. As the etching time was increased to 2 min, there was no observable change in the above-mentioned 'hot-spots' (Fig. 1c). However, novel 'hot-spots' were fabricated on the glass substrate; these consisted of unique 3-split ring arrays composed of 3 elliptical Ag dots (see Fig. S3, ESI†), which could not be formed for the case of the as-prepared raw FCC sample because of the limitation of the hole size.[3] Such metallic nanoarrays enhanced the Raman signals derived from the strong local EM field enhancement in the inter-particle regions.[3–9] The SERS intensity increased sharply with increase in the etching time from 2 min to 3 min. This remarkable enhancement was caused by the presence of nanotip arrays with sharp edges, which can themselves enhance the SERS intensity, leading to strong enhancement of the magnitude of EM fields (Fig. 1d).[10–16] The Raman intensity was decreased for the substrate produced using 4 min of SF_6 etching, despite the higher sharpness compared with the 3 min etched nanotip arrays (Fig. 1e). This reduction in intensity can be attributed to the change in nanotip geometry, from a triangular pyramidal shape to a conical shape, as shown in Fig. 2c and d. Not only the sharpness but also the shape and the number of resulting sharp corners also affect predominantly SERS activities.[10–16] For the triangular pyramidal nanotips, four sharp corners existed. However, the conical nanotips had only 1 sharp corner, and circular edges; these could also act as 'hot-spots', but the effect was relatively weaker and inefficient.[10,16] Hence, the SERS signals became weaker as the etching time was increased from 3 min to 4 min.

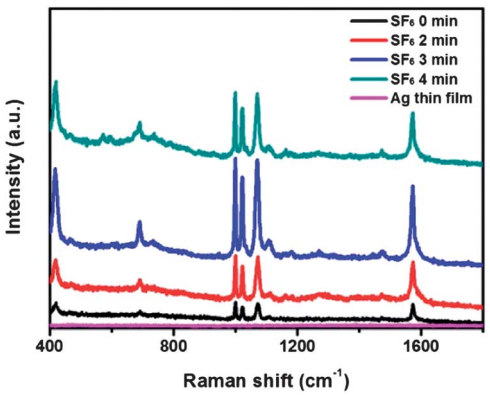

Fig. 3 SERS spectra of BT-adsorbed nanotip arrays produced under various SF_6 RIE conditions, with an Ag thin film as the reference.

Another important factor for SERS applications—the uniform sensitivity of the SERS substrate over large areas—was also tested (see Fig. S4, ESI†). We obtained very similar SERS intensities for the characteristic peaks of BT from nine points randomly selected in the same sample (a 3 min etched substrate with a directionally deposited 25 nm Ag film). A 6.3% standard deviation was calculated from the peak height at 1017 cm^{-1}, which is an unprecedentedly small value compared with previously reported SERS substrates.[6–16]

To obtain the finer-scale surface roughness on the nanotip arrays, additional O_2 RIE was performed on the polymeric nanotip arrays produced after the SF_6 RIE process. Fig. 4a illustrates the effects of the O_2 RIE in creating the surface roughness. In contrast with the substrate subjected only to SF_6 RIE (SEM image on the left), the additional application of O_2 RIE produced a surface with sub-40 nm gaps (right-hand SEM image), with no effect on the overall tip shape. Actually, the reasons of roughening need further investigation, including the study of the effects of etchant shadowing and first-order re-emission.[6,26,27] The polymeric, dual length-scale, O_2 plasma-etched nanotip arrays were relatively well-fabricated over a large area, as shown in Fig. 4b. To maximize the roughness effect for subsequent sensing applications, we changed the metal deposition method from electron-beam evaporation (directional deposition) to multi-sputtering (isotropic deposition). Fig. 4c and d show SEM images of the resulting metallic dual length-scale nanotip arrays, created *via* the deposition of a thin Ag film (10 nm) using the as-prepared 3 min SF_6 etched substrate, which exhibited highly enhanced Raman signals (Fig. 3). The roughness of the Ag-deposited tip surface and nano-trenches with sub-15 nm gaps on the side-walls are clearly observed in these images, in contrast with that of the SF_6 etched substrate without any O_2 plasma treatment (see Fig. S5, ESI†).

To study the effects of this roughness for SERS-based sensing applications, Raman sensitivities were measured using the same experimental conditions as those described above. The effects of the finer length scale surface-roughness on the signal enhancement are shown in Fig. 5a. The combined SERS-enhancing effects of the sharp tips and the roughness (which could form nano-trenches with sub-15 nm gaps) of the dual length-scale nanotips led to a more than two-fold increase in the Raman

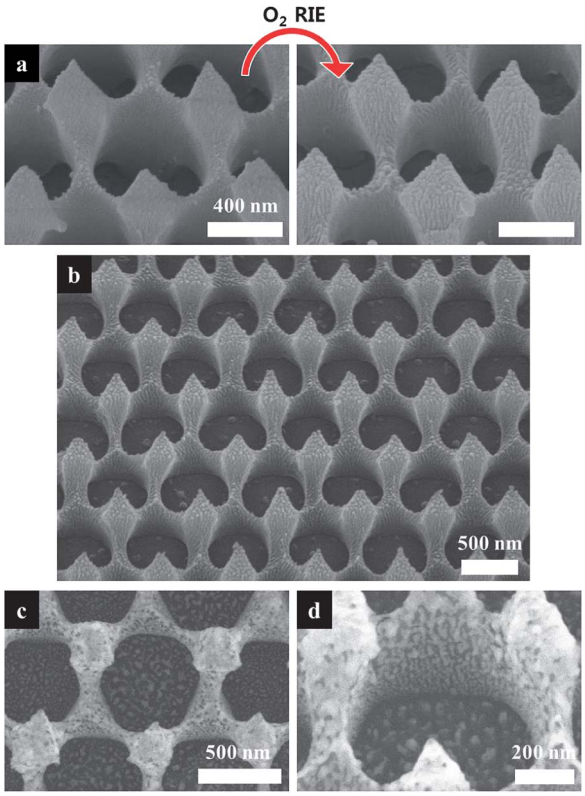

Fig. 4 (a) SEM images of the triangular pyramid-shaped nanotip arrays before (left) and after (right) additional O_2 RIE. (b) Large-area SEM image of the fabricated hexagonally ordered, dual length-scale nanotip arrays. (c) SEM image of the triangular pyramid-shaped dual length-scale nanotip arrays, after the isotropic deposition of an Ag thin film in the (111) plane. (d) Magnified 30° tilted SEM image of (c).

intensity, compared with the case where only the sharp-tip enhancement effect was present. Based on the spectrum obtained, the Raman enhancement factor (EF) at 1071 cm^{-1} could be calculated from the following equation:

$$EF = I_{SERS}/I_{Ref} \times N_{Ref}/N_{SERS},$$

where I_{SERS} and I_{Ref} are the Raman intensities of the band 1071 cm^{-1} from the resulting SERS substrate and the reference, respectively, and N_{SERS} and N_{Ref} are the number of molecules in the spots of the illuminating laser (1 μm) on the surface and in the bulk solution, respectively. In this study, a bulk solution of 99% BT on a glass substrate was used as the reference.[5] As a result, the analytical Raman EF of the dual length-scale nanotip at 1071 cm^{-1} is 4.2×10^7, which is comparable to previously reported values.[6,10–16] The large-scale sample homogeneity of these SERS substrates was reasonably good, as demonstrated by the 7.6% standard deviation measured from the peak height at 1017 cm^{-1} (Fig. 5b). We believe that the increase in the standard deviation (compared with that measured before O_2 RIE was performed; an increase from 6.3% to 7.6%) was due to the characteristics of O_2 plasma etching, where the random etching of the polymeric nanotip surface caused a slightly different density of 'hot-spots'.[6] An important issue for fabricating SERS substrates is the reproducibility as well as the uniformity. Prism HL can easily create defect-free 3D structures with sub-micrometer scale

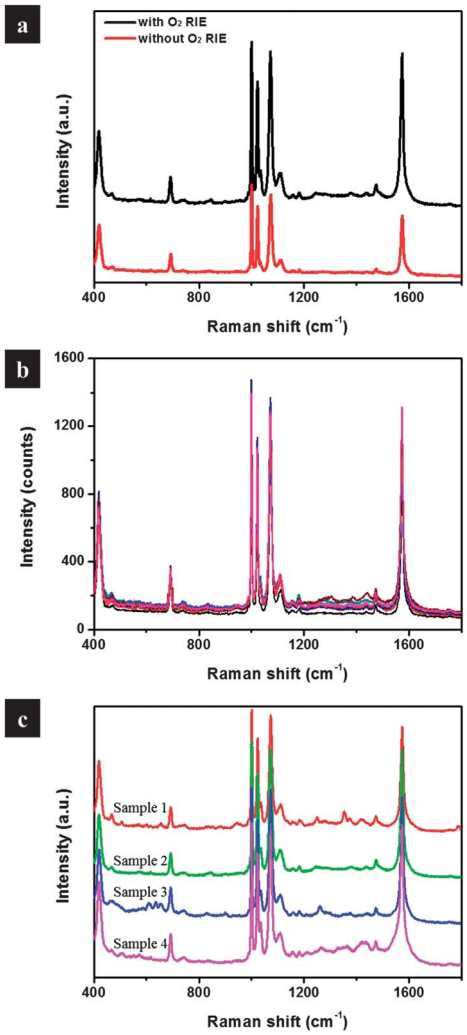

Fig. 5 (a) Comparison between the SERS spectra obtained for BT adsorbed onto metallic nanotip arrays with and without nanoroughness. SERS spectra of BT obtained from nine randomly selected spots on the triangular pyramid-shaped dual length-scale nanotip arrays (b) and four different dual length-scale nanotip array samples (c). Data acquisition involved 5 s accumulation.

periodicity over a large area within a second of laser exposure.[3,19–21] As demonstrated in Fig. 5c, the fairly uniform Raman intensities could be obtained from four different samples of dual length-scale nanotip arrays.

Furthermore, the roughened regions of the dual length-scale nanotip arrays showed potential as a fluorescence-based sensing platform.[4–6] Fig. 6 shows the fluorescent intensity profile after the as-prepared sample was immersed in a 10 μM R6G solution for 20 min; the profile was taken by horizontal scanning of the confocal microscope inset image of Fig. 6. This result indicated that the roughened regions of the dual length-scale nanotips (a large equilateral triangle area with 0.4 cm side in length with red color) gave highly intensified fluorescence signals compared with the flat Ag surface (black area) for 15 min under laser irradiation (see Fig. S6, ESI†). With increase in the laser irradiation time, the fluorescence intensity decreased because of photodegradation of the adsorbed dye molecules. This intensification was likely derived from the increased adsorption capacity for

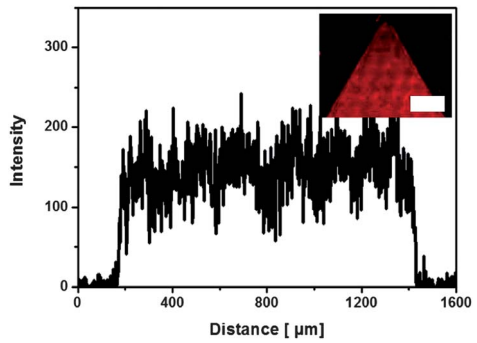

Fig. 6 R6G fluorescent intensity profile for the resulting dual length-scale nanotip arrays (R6G concentration was 10 μM). The inset shows a large-area confocal microscope image of R6G-adsorbed triangular pyramid-shaped dual length-scale nanotip arrays, and a flat Ag film. The scale bar represents 400 μm.

target molecules (R6G) afforded by the enlarged surface area compared with either the flat Ag thin film or the sharp tip arrays (without nanoscale roughness) under the same experimental conditions (see Fig. S6, ESI†).[4–6]

Conclusions

In summary, we have reported a facile method for the fabrication of large-area, hexagonally ordered nanotip arrays with controllable morphological features—including the sharpness, shape, and roughness—through the combination of prism HL, RIE, and a metal deposition process. The overall shape of the polymeric nanotip arrays was changed from triangular pyramidal to conical, where the increased sharpness was produced by increasing the SF_6 etching time (from 3 min to 4 min). After the application of a directional Ag deposition process, the metallic nanostructure arrays showed tunable SERS activities as a function of the etching duration, and large-scale sample homogeneity. Furthermore, small-scale surface roughness could be produced in the polymeric nanotips by the application of additional O_2 RIE; this created more 'hot-spots' after the isotropic deposition of Ag on the dual length-scale nanotips, resulting in further enhancement of the already improved Raman signals. Finally, the potential of the dual length-scale nanotip arrays for fluorescence-based sensing was verified. Such metallic nanostructures are expected to be useful for chemical and biomolecular sensing, when incorporated into microfluidic devices *via* integration with conventional photo-lithography.[19,20]

Acknowledgements

This work was supported by a grant from the Creative Research Initiative Program of the Ministry of Education, Science and Technology for "Complementary Hybridization of Optical and Fluidic Devices for Integrated Optofluidic Systems." Partial support from the Brain Korea 21 Program is also appreciated.

Notes and references

1 C. L. Haynes, A. D. McFarland and R. P. Van Duyne, *Anal. Chem.*, 2005, **77**, 338a.
2 K. Kneipp, *Phys. Today*, 2007, **60**, 40.
3 H. C. Jeon, C. J. Heo, S. Y. Lee, S. G. Park and S. M. Yang, *J. Mater. Chem.*, 2012, **22**, 4603.
4 H. C. Jeon, C. J. Heo, S. Y. Lee and S. M. Yang, *Adv. Funct. Mater.*, 2012, **22**, 4268.
5 H. C. Jeon, S. G. Han, S. G. Park and S. M. Yang, *RSC Adv.*, 2012, **2**, 2334.
6 L. Y. Wu, B. M. Ross, S. Hong and L. P. Lee, *Small*, 2010, **6**, 503.
7 S. K. Yang, W. P. Cai, L. C. Kong and Y. Lei, *Adv. Funct. Mater.*, 2010, **20**, 2527.
8 N. A. Hatab, C. H. Hsueh, A. L. Gaddis, S. T. Retterer, J. H. Li, G. Eres, Z. Y. Zhang and B. H. Gu, *Nano Lett.*, 2010, **10**, 4952.
9 L. Gunnarsson, E. J. Bjerneld, H. Xu, S. Petronis, B. Kasemo and M. Kall, *Appl. Phys. Lett.*, 2001, **78**, 802.
10 Y. Lu, G. L. Liu, J. Kim, Y. X. Mejia and L. P. Lee, *Nano Lett.*, 2005, **5**, 119.
11 V. Guieu, F. L. Lagugne-Labarthet, L. Servant, D. Talaga and N. Sojic, *Small*, 2008, **4**, 96.
12 Y. Hirai, H. Yabu, Y. Matsuo, K. Ijiro and M. Shimomura, *Chem. Commun.*, 2010, **46**, 2298.
13 Y. Yang, Z. Y. Li, K. Yamaguchi, M. Tanemura, Z. R. Huang, D. L. Jiang, Y. H. Chen, F. Zhou and M. Nogami, *Nanoscale*, 2012, **4**, 2663.
14 A. M. Bowen, M. J. Motala, J. M. Lucas, S. Gupta, A. J. Baca, A. Mihi, A. P. Alivisatos, P. V. Braun and R. G. Nuzzo, *Adv. Funct. Mater.*, 2012, **22**, 2927.
15 H. H. Cheng, S. W. Chen, Y. Y. Chang, J. Y. Chu, D. Z. Lin, Y. P. Chen and J. H. Li, *Opt. Express*, 2011, **19**, 22125.
16 N. C. Linn, C. H. Sun, A. Arya, P. Jiang and B. Jiang, *Nanotechnology*, 2009, **20**, 225303.
17 L. J. Wu, Y. C. Zhong, C. T. Chan, K. S. Wong and G. P. Wang, *Appl. Phys. Lett.*, 2005, **86**, 241102.
18 Y. K. Pang, J. C. W. Lee, C. T. Ho and W. Y. Tam, *Opt. Express*, 2006, **14**, 9113.
19 S. K. Lee, S. G. Park, J. H. Moon and S. M. Yang, *Lab Chip*, 2008, **8**, 388.
20 S. G. Park, S. K. Lee, J. H. Moon and S. M. Yang, *Lab Chip*, 2009, **9**, 3144.
21 S. G. Park, J. H. Moon, S. K. Lee, J. Shim and S. M. Yang, *Langmuir*, 2010, **26**, 1468.
22 M. Campbell, D. N. Sharp, M. T. Harrison, R. G. Denning and A. J. Turberfield, *Nature*, 2000, **404**, 53.
23 J. H. Moon, J. Ford and S. Yang, *Polym. Adv. Technol.*, 2006, **17**, 83.
24 J. H. Jang, C. K. Ullal, M. Maldovan, T. Gorishnyy, S. Kooi, C. Y. Koh and E. L. Thomas, *Adv. Funct. Mater.*, 2007, **17**, 3027.
25 S. G. Park, J. H. Moon, H. C. Jeon and S. M. Yang, *Soft Matter*, 2012, **8**, 4567.
26 J. T. Drotar, Y. P. Zhao, T. M. Lu and G. C. Wang, *Phys. Rev. B: Condens. Matter*, 2000, **61**, 3012.
27 J. T. Drotar, Y. P. Zhao, T. M. Lu and G. C. Wang, *Phys. Rev. B: Condens. Matter*, 2000, **62**, 2118.

